Research Square

Preprints are preliminary reports that have not undergone peer review.
They should not be considered conclusive, used to inform clinical practice,
or referenced by the media as validated information.

TNF-α Induces CCL28-Mediated Recruitment of Th22 Cells in Hepatocellular Carcinoma

Jingsong Huang
Wuhan City Sixth Hospital: Affiliated Hospital of Jianghan University
Yilin Li
2879035410qq.com

Wuhan City Sixth Hospital: Affiliated Hospital of Jianghan University
Qing Yang
Baoshan People's Hospital
Lan Huang
Wuhan City Sixth Hospital: Affiliated Hospital of Jianghan University
Fan Ding
Wuhan City Sixth Hospital: Affiliated Hospital of Jianghan University
Qiang Tian
Wuhan City Sixth Hospital: Affiliated Hospital of Jianghan University
Shenzong Rao
Tongji Medical College of HUST: Huazhong University of Science and Technology Tongji Medical College Tongji Hospital https://orcid.org/0009-0003-7793-3917
Yanqiong Rao
Tongji Medical College of HUST: Huazhong University of Science and Technology Tongji Medical College Tongji Hospital

Research Article

Keywords: Hepatocellular carcinoma, Th22 cells, CCL28, CCR10, NF-κB, Tumor microenvironment

Posted Date: November 1st, 2026

DOI: https://doi.org/10.21203/rs.3.rs-10708836/v1

License: This work is licensed under a Creative Commons Attribution 4.0 International License.
Read Full License

Abstract

Background

The occurrence and development of hepatocellular carcinoma (HCC) are closely associated with the imbalance of the inflammatory and immune microenvironment. However, the regulatory mechanisms governing Th22 cell infiltration in HCC remain incompletely understood. This study aimed to investigate the molecular mechanism by which HCC cells recruit Th22 cells.

Methods

Peripheral blood mononuclear cells were isolated from healthy controls and newly diagnosed HCC patients, and subjected to flow cytometry, qPCR, Western blotting, chromatin immunoprecipitation, and Transwell migration assays.

Results

The results demonstrated that the proportion of naive $CD4^+$ T cells in the peripheral blood of HCC patients was significantly lower than that in healthy controls, whereas the proportions of Th22 cells and CCL28 levels were markedly elevated. TNF-α induced the differentiation of naive $CD4^+$ T cells into Th22 cells and upregulated the transcription and protein expression of CCR10 in HCC cells (HepG2) and T cells (Jurkat) in a concentration-dependent manner; this effect was independent of changes in CCR10 protein degradation rates. Mechanistically, TNF-α activated the NF-κB signaling pathway, promoting the nuclear translocation of the p65 subunit. Chromatin immunoprecipitation and dual-luciferase reporter assays confirmed that activated p65 directly bound to specific sites within the CCR10 promoter region, thereby regulating its expression at the transcriptional level. Functional experiments revealed that HCC cells recruited CCR10-expressing Th22 cells via high CCL28 expression, an effect significantly inhibited by knocking down CCL28 or neutralizing CCR10.

Conclusion

This study is the first to elucidate the molecular mechanism by which the TNF-α/NF-κB/CCR10-CCL28 axis mediates the recruitment of Th22 cells by HCC cells. It reveals a positive feedback loop of "inflammatory cytokines–chemokines–immune cell recruitment" and provides a new theoretical basis for understanding the immune microenvironment in HCC, as well as potential novel targets for its diagnosis and targeted therapy.

Introduction

Hepatocellular carcinoma (HCC) is one of the most prevalent malignant tumors worldwide. As a region with a high incidence of HCC, China accounts for over half of the global new cases and deaths, compounded by a nationwide reservoir of approximately 75 million HBV-infected individuals, presenting a severe prevention and control scenario[1–4]. The pathogenesis of HCC results from complex interactions between genetic mutations in hepatocytes and the microenvironment, with 90% of cases accompanied by chronic uncontrollable inflammation[5]. The imbalance of the inflammatory-immune microenvironment is a core driver of tumor evolution.

Chemokines and their receptors form regulatory networks that play pivotal roles in tumor invasion, metastasis, and angiogenesis by mediating immune cell recruitment and activation, making them a hotspot in tumor microenvironment research[6,7]. Th22 cells, a recently identified subset of $CD4^+$ helper T cells, characteristically express CCR6, CCR10, and the skin-homing receptor CLA[8]. They specifically secrete IL-22 and participate in tissue repair and tumorigenesis by activating pathways such as STAT3 and MAPK, exerting a "double-edged sword" effect[9–11]. Emerging evidence suggests a close correlation between Th22 cells and HCC progression; for instance, $B7\text{-}H1^+$ antigen-presenting cells can accelerate hepatocarcinogenesis by promoting Th22 polarization via the PD-1 pathway[12]. Nevertheless, the recruitment mechanisms of Th22 cells within local HCC tissues and their interaction patterns with HCC cells remain to be fully elucidated.

TNF-α is a core inflammatory cytokine in the HCC microenvironment that can establish an inflammatory positive feedback loop by activating the NF-κB pathway[13]. The NF-κB pathway has been confirmed to regulate the transcription of various chemokine receptors[14]. CCL28, the characteristic ligand for CCR10, has been reported to mediate regulatory T cell recruitment and promote angiogenesis in HCC under hypoxic conditions[15]. However, whether it participates in the chemotactic recruitment of Th22 cells remains unclear. Based on this, the present study focused on the TNF-α/NF-κB/CCR10-CCL28 axis to explore the mechanism by which HCC cells recruit Th22 cells. We aimed to refine the regulatory network of the inflammatory-immune environment in HCC and provide potential new targets for immunotherapy.

Materials and Methods

Cell Culture and Transfection

HEK 293T, Jurkat, and HepG2 cells (obtained from the American Type Culture Collection [ATCC]) were cultured in Dulbecco's Modified Eagle Medium (Gibco, Shanghai, China) supplemented with 10% fetal bovine serum (Gibco) at 37°C in a 5% CO_2 atmosphere. Cells were seeded into 6-well plates (4×10^5 cells/well) or 12-well plates (2×10^5 cells/well) and grown to approximately 70% confluence prior to transfection. siRNA was transfected into cells using Lipofectamine 2000 reagent (Invitrogen, Shanghai, China).

Western Blot Analysis

Cells were lysed in RIPA buffer containing SDS. Protein samples were separated by SDS-polyacrylamide gel electrophoresis (PAGE) and transferred onto nitrocellulose membranes (Pall). Membranes were blocked with skim milk and incubated with primary antibodies: anti-p65 (Servicebio), anti-β-actin (Proteintech, Wuhan), anti-Histone H3 (Immunoway), anti-CCR10 (Proteintech, Wuhan), followed by horseradish peroxidase (HRP)-conjugated AffiniPure Goat Anti-Rabbit IgG (H + L) or HRP-conjugated AffiniPure Goat Anti-Mouse IgG (H + L) (Proteintech, Wuhan). Immunoreactive bands were visualized using an Enhanced Chemiluminescence (ECL) substrate (Thermo Fisher Scientific).

Enzyme-Linked Immunosorbent Assay (ELISA)

Collected cell supernatants were thawed, and CCL28 concentrations were measured using a commercial ELISA kit according to the manufacturer's instructions.

Immunofluorescence

Cells were cultured on glass coverslips and treated with TNF-α or shRNA. After washing twice with PBS, cells were fixed with 4% paraformaldehyde for 15 min, followed by three 5-min washes with PBS. Permeabilization was performed with 0.1% Triton X-100 for 10 min, and non-specific binding sites were blocked with 1% bovine serum albumin (BSA) in PBS for 30 min at room temperature. Cells were then incubated overnight at 4°C with primary antibodies (Beyotime), washed three times with PBS, and subsequently incubated with secondary antibodies (Beyotime) at 37°C for 50 min. Finally, cells were permeabilized again, counterstained with DAPI, and mounted for microscopy.

Quantitative Real-Time PCR (qPCR)

Total mRNA was extracted using TRIzol reagent according to the manufacturer's protocol. One microgram of mRNA was used as a template for reverse transcription PCR in a 20 μL reaction system containing 2× cDNA Synthesis SuperMix (10 μL), gDNA Purge (1 μL), and nuclease-free water. Reaction conditions were: 50°C for 15 min, 85°C for 5 sec, and hold at 4°C. Real-time PCR was performed in a 20 μL reaction mix containing 2× SYBR Select Master Mix and specific primers. Cycling conditions included initial denaturation at 95°C for 1 min; 40 cycles of denaturation at 95°C for 15 sec, annealing/extension at 60°C for 1 min; followed by a default melt curve analysis.

Dual-Luciferase Reporter Assay

Dual-luciferase reporter assays were conducted using a Dual-Luciferase Reporter Assay Kit II (Beyotime). Briefly, cells were seeded into 6-well plates (2×10^5 cells/well). For transfection, 2 μg of plasmid DNA was diluted in 100 μL of serum-free opti-MEM for each sample and transfected for 6 hours. Subsequently, cells were processed using the Dual-Luciferase Reporter Assay Kit II, and relative light units (RLU) were measured.

Th22 Cell Migration Assay

Human peripheral blood mononuclear cells were isolated, and $CD4^+$ cells were sorted to prepare single-cell suspensions. Transwell assays were conducted with the following experimental groups: Control group (upper chamber: 100 μL $CD4^+$ cells; lower chamber: 300 μL normal hepatocytes LO2); HCC group (upper chamber: 100 μL $CD4^+$ cells; lower chamber: 300 μL HepG2 cells); siNC group (upper chamber: 100 μL $CD4^+$ cells; lower chamber: 300 μL HepG2 cells + siNC); si-CCL28 group (upper chamber: 100 μL $CD4^+$ cells; lower chamber: 300 μL HepG2 cells + si-CCL28); CCR10 neutralizing antibody group (upper chamber: 100 μL $CD4^+$ cells pre-incubated with 10 μL CCR10 neutralizing antibody for 1 h; lower chamber: 300 μL HepG2 cells); CCR10 isotype control group (upper chamber: 100 μL $CD4^+$ cells pre-incubated with 10 μL CCR10 isotype control antibody; lower chamber: 300 μL HepG2 cells); CCR10 neutralizing antibody + si-CCL28 group (upper chamber: 100 μL $CD4^+$ cells pre-incubated with 10 μL CCR10 neutralizing antibody; lower chamber: 300 μL HepG2 cells + si-CCL28); CCR10 neutralizing antibody + siNC group (upper chamber: 100 μL $CD4^+$ cells pre-incubated with 10 μL CCR10 isotype control antibody; lower chamber: 300 μL HepG2 cells + siNC). After incubation, migrated cells in the lower chamber were collected for phenotypic identification and counting via flow cytometry.

Flow Cytometry

Human-derived antibodies used included: anti-CD45RA, anti-CD4, anti-CCR6, anti-CCR4, and anti-CCR10 (all purchased from BD Biosciences). Flow cytometric analysis was performed on a CytoFLEX S flow cytometer (Beckman Coulter).

Medical Ethics

This study was approved by the relevant Ethics Committee (Approval No. WHSHIRB-K-2024012). All experimental procedures complied with the Declaration of Helsinki and relevant laws and regulations. Written informed consent was obtained from all participants prior to peripheral blood sample collection. We are committed to protecting participant privacy; all data were anonymized, and no personally identifiable information is included in this manuscript.

Results

TNF-α Promotes the Differentiation of Naive $CD4^+$ T Cells into Th22 Cells

To investigate the dynamics of naive $CD4^+$ T cells and Th22 cells upon TNF-α stimulation, we isolated peripheral blood mononuclear cells from healthy volunteers and newly diagnosed HCC patients and sorted $CD4^+$ T cells. Flow cytometry with double staining ($CD45RA^+/CD45RO^-$) was employed to identify the proportion of naive $CD4^+$ T cells, while triple staining (CCR4/CCR6/CCR10) was used to identify Th22 cells. The results showed that the proportion of naive $CD4^+$ T cells in healthy individuals (Fig. 1A) was significantly higher than that in HCC patients, whereas the proportion of Th22 cells (Fig. 1B) was notably lower. Furthermore, stimulating healthy human peripheral blood cells with TNF-α led to a significant decrease in the proportion of naive $CD4^+$ T cells (Fig. 1C) and a marked increase in Th22 cells (Fig. 1D).

These data suggest that TNF-α induces the differentiation of naive $CD4^+$ T cells into Th22 cells. Given that Th22 cells can also secrete TNF-α, this process may establish a positive feedback loop sustaining Th22 differentiation. Concurrently, ELISA analysis revealed that plasma CCL28 levels in HCC patients were significantly higher than those in healthy controls (Fig. 1E). Similarly, TNF-α stimulation elevated CCL28 levels in the supernatant of healthy donor cultures (Fig. 1E), indicating that HCC cells exhibit high CCL28 expression.

TNF-α Upregulates CCR10 Expression in Th22 Cells

Given that TNF-α induces the differentiation of naive $CD4^+$ T cells into Th22 cells, which characteristically express CCR10, we hypothesized that TNF-α might concurrently regulate CCR10 expression. To test this, we assessed CCR10 expression in HepG2 and Jurkat cells following stimulation with varying concentrations of TNF-α. qPCR results demonstrated a significant, concentration-dependent upregulation of CCR10 transcription in both HepG2 (Fig. 2A) and Jurkat (Fig. 2B) cells. Western blot analysis corroborated these findings, showing increased CCR10 protein levels correlating with TNF-α concentration (Fig. 2C, 2D).

To exclude the possibility that enhanced CCR10 protein expression resulted from impaired degradation, we treated HepG2 (Fig. 2E) and Jurkat (Fig. 2F) cells with cycloheximide (CHX) to inhibit protein synthesis and monitored CCR10 dynamics via Western blotting to plot protein degradation half-life curves. No significant difference in CCR10 protein half-life was observed between the groups, indicating that TNF-α-induced CCR10 upregulation is not mediated by increased protein stability. In summary, TNF-α promotes CCR10 expression in $CD4^+$ T cells at the transcriptional level.

Activated p65 in the NF-κB Pathway Directly Regulates CCR10 Expression

TNF-α is a key activator of the NF-κB signaling pathway; thus, we hypothesized that it promotes CCR10 expression via NF-κB activation. We first examined NF-κB activation following TNF-α stimulation. Western blot analysis of nuclear proteins for phosphorylated p65 revealed accumulation of p65 in the nucleus and a concomitant reduction in the cytoplasm in both HepG2 (Fig. 3A) and Jurkat (Fig. 3B) cells. Immunofluorescence further validated the subcellular localization shift: in HepG2 cells, TNF-α stimulation prompted the translocation of p65 from the cytoplasm to the nucleus (Fig. 3C), confirming effective NF-κB pathway activation by TNF-α.

To delineate the regulatory role of NF-κB on CCR10, we designed and transfected shRNA targeting p65 to knock down its expression. PCR analysis confirmed efficient p65 knockdown in both HepG2 (Fig. 3D) and Jurkat (Fig. 3E) cells. Under this condition, cells were stimulated with TNF-α and CCR10 expression was assessed. Knockdown of p65 resulted in reduced nuclear p65 and increased cytoplasmic p65, as observed by Western blot and immunofluorescence (Fig. 3F-H). Concurrently, qPCR showed significant decreases in CCR10 mRNA levels in both cell lines (Fig. 3I-J). These results confirm the involvement of the NF-κB signaling pathway in regulating CCR10 expression.

To verify whether activated p65 directly acts on the CCR10 promoter, we utilized the JASPAR database to predict potential binding sites within the CCR10 promoter region (2000 bp upstream of the transcription start site) (Fig. 3K) and designed primers for chromatin immunoprecipitation (ChIP) assays. In Jurkat cells, primer 1, designed against a predicted binding site, effectively enriched the target DNA fragment (Fig. 3L). Concurrent Western blotting confirmed the presence of p65 in the immunoprecipitated complexes (Fig. 3M). Furthermore, we constructed four pGL3-Basic luciferase reporter vectors carrying different mutations within the CCR10 promoter region. Luciferase activity assays indicated that mutant 1 exhibited significantly reduced activity compared to the wild-type promoter (Fig. 3N). Transfection of pGL3/CCR10 and pGL3/CCR10 mut vectors into HepG2 and Jurkat cells, alongside an NF-κB overexpression plasmid, revealed significantly decreased luciferase activity in cells transfected with the mutant constructs (Fig. 3O). These data demonstrate that upon TNF-α activation of the NF-κB pathway, activated p65 directly binds to the CCR10 promoter region to regulate its expression transcriptionally.

HCC Cells Recruit Th22 Cells via CCL28

Previous reports indicate that HCC cells upregulate CCL28 under hypoxia to recruit regulatory T cells and promote angiogenesis[15]. We hypothesized that TNF-α-stimulated HCC cells might similarly recruit Th22 cells via CCL28. To validate this, we constructed CCL28-knockdown (CCL28-KD) HepG2 cell lines via transient transfection with targeted siRNA, and qPCR confirmed significant knockdown efficiency (Fig. 4A). Human peripheral blood mononuclear cells were isolated, and $CD4^+$ T cells were seeded in the upper chamber of Transwell inserts. The lower chambers contained various treatments: normal hepatocytes, HCC cells, CCL28 neutralizing antibody, isotype control antibody, combined with CCL28 siRNA or CCR10 neutralizing antibody. Flow cytometry was employed to analyze migrated T cell subsets in the lower chamber, specifically quantifying the chemotactic capacity of HCC cells toward Th22 cells within PBMCs. Compared to the normal hepatocyte group, the presence of HCC cells in the lower chamber recruited significantly more Th22 cells. This recruitment was substantially diminished upon treatment with si-CCL28 or CCR10 neutralizing antibody. Combined blockade using both si-CCL28 and CCR10 neutralizing antibody yielded a similar inhibitory effect. These results confirm that HCC cells specifically recruit CCR10-expressing Th22 cells through the secretion of CCL28.

Discussion

This study focused on the core regulatory mechanisms of the inflammatory-immune microenvironment in HCC and is the first to systematically elucidate the TNF-α/NF-κB/CCR10-CCL28 axis as a mediator of Th22 cell recruitment by HCC cells, offering a fresh perspective on tumor-immune cell interactions. We initially observed that newly diagnosed HCC patients exhibit significantly lower proportions of circulating naive $CD4^+$ T cells but higher proportions of Th22 cells and elevated CCL28 levels compared to healthy controls. In vitro experiments further confirmed that TNF-α induces the differentiation of naive $CD4^+$ T cells into Th22 cells. Moreover, the TNF-α secreted by Th22 cells themselves likely establishes a positive feedback loop, amplifying this differentiation effect—a phenomenon consistent with the expansion of

Th22 cells observed in various solid tumors, including lung and colorectal cancers[16,17], suggesting that Th22 accumulation may be a common feature of the HCC microenvironment.

The mechanistic insights represent a core innovation of this research: we defined the upstream signaling and transcriptional regulation of CCR10 by TNF-α. In both HepG2 and Jurkat cells, TNF-α activates the NF-κB pathway, driving p65 nuclear translocation. shRNA-mediated p65 knockdown significantly reduced CCR10 transcription and protein levels without affecting protein half-life, ruling out post-translational modifications. Subsequent ChIP and dual-luciferase reporter assays provided direct evidence that activated p65 binds to specific sites within the CCR10 promoter to drive its transcription. This finding not only expands the downstream regulatory network of NF-κB but also provides novel evidence regarding the transcriptional control of chemokine receptors—while previous studies predominantly focused on NF-κB's regulation of ligands like CCL27 and CCL28[13,15,18], our work highlights its direct regulatory role on the receptor, CCR10.

Based on the ligand-receptor pairing of CCR10 and CCL28, we uncovered the functional mechanism of Th22 recruitment by HCC cells: HCC cells' high expression of CCL28 serves as the key effector molecule mediating Th22 chemotaxis, as evidenced by the significant reduction in Th22 migration upon CCL28 knockdown or CCR10 neutralization. This conclusion resonates strongly with prior reports of CCL28 recruiting regulatory T cells under hypoxic conditions, suggesting that CCL28, as a chemokine, can selectively recruit distinct functional T cell subsets depending on microenvironmental cues (e.g., hypoxia, inflammatory stimuli), thereby collectively shaping an immunosuppressive niche. Notably, recruited Th22 cells secrete TNF-α, which further upregulates CCR10 and CCL28 expression in both autologous cells and HCC cells, establishing a "cytokine–chemokine–immune cell recruitment" positive feedback loop that perpetuates tumor progression.

The clinical implications of our study lie in identifying the Th22-associated chemotactic axis as a potential diagnostic and therapeutic target for HCC. Firstly, the elevated levels of Th22 cells and CCL28 in the peripheral blood of HCC patients suggest their utility as complementary biomarkers for early HCC diagnosis. Secondly, targeting the CCR10-CCL28 interaction could potentially block Th22 recruitment and remodel the tumor microenvironment—offering a promising strategy to overcome resistance in current immunotherapies. Admittedly, this study has limitations: current findings are primarily based on cellular assays and peripheral blood samples. Future validation is required to correlate Th22 infiltration and CCR10/CCL28 expression with clinicopathological features in matched HCC and paracancerous tissues. Additionally, in vivo models are necessary to ascertain the physiological relevance of this axis and evaluate the therapeutic potential of targeted interventions. Furthermore, the precise mechanisms by which recruited Th22-derived IL-22 regulates HCC proliferation and metastasis, and its crosstalk with other immune subsets, warrant deeper investigation.

Conclusions

The elucidation of the TNF-α/NF-κB/CCR10-CCL28 axis in this study refines the regulatory network of the HCC immune microenvironment and provides a theoretical foundation for developing intervention strategies targeting Th22 recruitment, potentially paving the way for novel immunotherapeutic approaches against HCC.

Declarations

Ethics approval and consent to participate

This study was conducted in accordance with the Declaration of Helsinki and approved by the Ethics Committee of the Sixth Hospital of Wuhan (Approval No. WHSHIRB-K-2024012). Informed consent was obtained from all subjects involved in the study.

Consent for publication
Not applicable. No identifiable personal information is included in this paper.

Availability of data and materials

All data generated or analysed during this study are included in this published article

Competing interests

The authors declare that they have no competing interests" in this section.

Funding

This research was funded by the Wuhan Municipal Health Commission (Project Number: WX23A38).

Author Contributions

JSH, SZR, and QY conceived and designed the experiments. FD and LH performed the cell-based experiments. QT analyzed the data. YLL and JSH drafted the manuscript.

Acknowledgments

Not applicable.

References

1. Siegel RL, Giaquinto AN, Jemal A, Cancer statistics. 2024. CA: A Cancer Journal for Clinicians 2024;74(1):12–49. doi: 10.3322/caac.21820. PMID.
2. Xia C, Dong X, Li H, Cao M, Sun D, He S et al., *Cancer statistics in China and United States, 2022: profiles, trends, and determinants. Chinese Medical Journal. 2022;135(5):584–590.* 10.1097/cm9.0000000000002108. *PMID*:

3. McGlynn KA, Petrick JL, El-Serag HB. Epidemiology of Hepatocellular Carcinoma. Hepatology. 2020;73(S1):4–13. 10.1002/hep.31288. PMID.
4. Deng Y, Meng T, You H, Jia J, Wang Y, Epidemiology. Achievements, and Challenges in the Elimination of Hepatitis B in China. J Clin Transl Hepatol 2025;13(7):599–604. 10.14218/jcth.2025.00039. PMID: 40937078.
5. Nakagawa H. Inflammation- and stress-related signaling pathways in hepatocarcinogenesis. World Journal of Gastroenterology. 2012;18(31) 10.3748/wjg.v18.i31.4071. PMID.
6. Balkwill F. Cancer and the chemokine network. Nature Reviews Cancer. 2004;4(7):540–550. 10.1038/nrc1388. PMID.
7. Zajkowska M, Mroczko B. Chemokines in Primary Liver Cancer. International Journal of Molecular Sciences. 2022;23(16) 10.3390/ijms23168846. PMID.
8. Mousset CM, Hobo W, Woestenenk R, Preijers F, Dolstra H, van der Waart AB. Comprehensive Phenotyping of T Cells Using Flow Cytometry. Cytometry Part A. 2019;95(6):647–654. 10.1002/cyto.a.23724. PMID.
9. Jiang Q, Yang G, Xiao F, Xie J, Wang S, Lu L et al., *Role of Th22 Cells in the Pathogenesis of Autoimmune Diseases. Frontiers in Immunology. 2021;12* 10.3389/fimmu.2021.688066. *PMID*:
10. Wang W, Sung N, Gilman-Sachs A, Kwak-Kim JT, Helper. (Th) Cell Profiles in Pregnancy and Recurrent Pregnancy Losses: Th1/Th2/Th9/Th17/Th22/Tfh Cells. Frontiers in Immunology 2020;11 10.3389/fimmu.2020.02025. PMID.
11. Zhang P, Liu J, Lee A, Tsaur I, Ohira M, Duong V et al., *IL-22 resolves MASLD via enterocyte STAT3 restoration of diet-perturbed intestinal homeostasis. Cell Metabolism. 2024;36(10):2341–2354.e2346.* 10.1016/j.cmet.2024.08.012. *PMID*:
12. Kuang D-M, Xiao X, Zhao Q, Chen M-M, Li X-F, Liu R-X et al., *B7-H1–expressing antigen-presenting cells mediate polarization of protumorigenic Th22 subsets. Journal of Clinical Investigation. 2014;124(10):4657–4667.* 10.1172/jci74381. *PMID*:
13. Vestergaard C, Johansen C, Otkjaer K, Deleuran M, Iversen L. Tumor necrosis factor-α-induced CTACK/CCL27 (cutaneous T-cell-attracting chemokine) production in keratinocytes is controlled by nuclear factor κB. Cytokine. 2005;29(2):49–55. 10.1016/j.cyto.2004.09.008. PMID.
14. DiDonato JA, Mercurio F, Karin M. NF-κB and the link between inflammation and cancer. Immunological Reviews. 2012;246(1):379–400. 10.1111/j.1600-065X.2012.01099.x. PMID.
15. Ren L, Yu Y, Wang L, Zhu Z, Lu R, Yao Z. Hypoxia-induced CCL28 promotes recruitment of regulatory T cells and tumor growth in liver cancer. Oncotarget. 2016;7(46):75763–75773. 10.18632/oncotarget.12409. PMID: 27716621.
16. Yao Y, Yang G, Lu G, Ye J, Cui L, Zeng Z et al., *Th22 Cells/IL-22 Serves as a Protumor Regulator to Drive Poor Prognosis through the JAK-STAT3/MAPK/AKT Signaling Pathway in Non-Small-Cell Lung Cancer. Journal of Immunology Research. 2022;2022:1–12.* 10.1155/2022/8071234. *PMID*:
17. Sun D, Wang W, Guo F, Pitter MR, Du W, Wei S et al., *DOT1L affects colorectal carcinogenesis via altering T cell subsets and oncogenic pathway. OncoImmunology. 2022;11(1)*

10.1080/2162402x.2022.2052640. *PMID*:

18. Karakawa M, Komine M, Hanakawa Y, Tsuda H, Sayama K, Tamaki K et al., *CCL27 Is Downregulated by Interferon Gamma via Epidermal Growth Factor Receptor in Normal Human Epidermal Keratinocytes. Journal of Cellular Physiology. 2014;229(12):1935–1945.* 10.1002/jcp.24643. *PMID*:

Figures

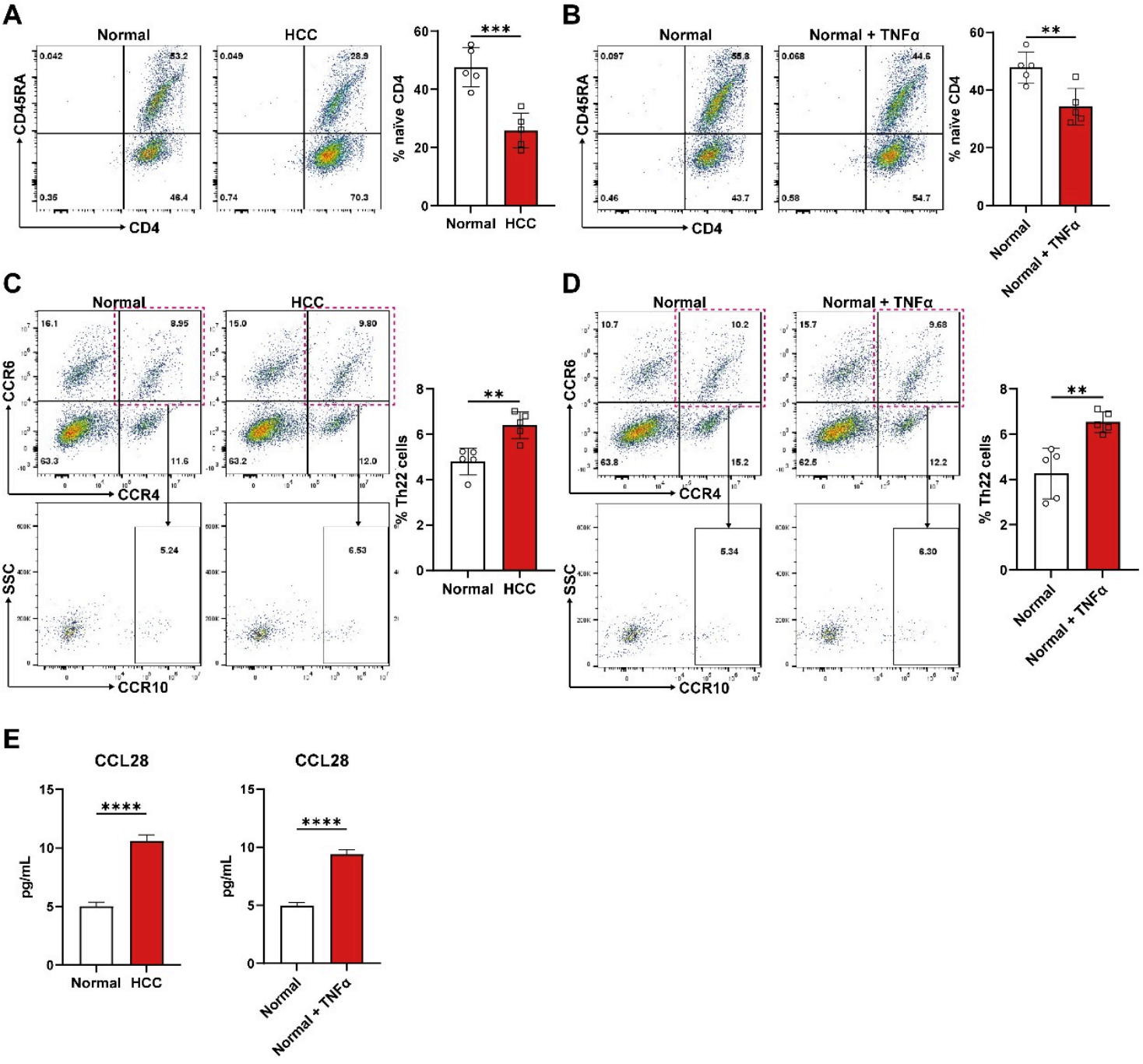


Figure 1

TNF-α promotes the differentiation of naive CD4⁺ T cells into Th22 cells and elevates CCL28 in HCC patients.

(A) Representative flow cytometry plots showing the proportion of naive CD4⁺ T cells (CD45RA⁺CD45RO⁻) in CD4⁺ T cells from healthy donors (HD) and newly diagnosed HCC patients. (B) Representative plots showing the proportion of Th22 cells (CCR4⁺CCR6⁺CCR10⁺) in CD4⁺ T cells from HD and HCC patients. (C,D) Naive CD4⁺T cells from HD were stimulated with TNF-α; naive CD4⁺ T cell proportion decreased (C) and Th22 cell proportion increased (D) compared with untreated controls. (E) ELISA quantification of plasma CCL28 levels in HD and HCC patients; CCL28 was significantly elevated in HCC. Data are representative of three independent experiments. *P < 0.05 vs. control.

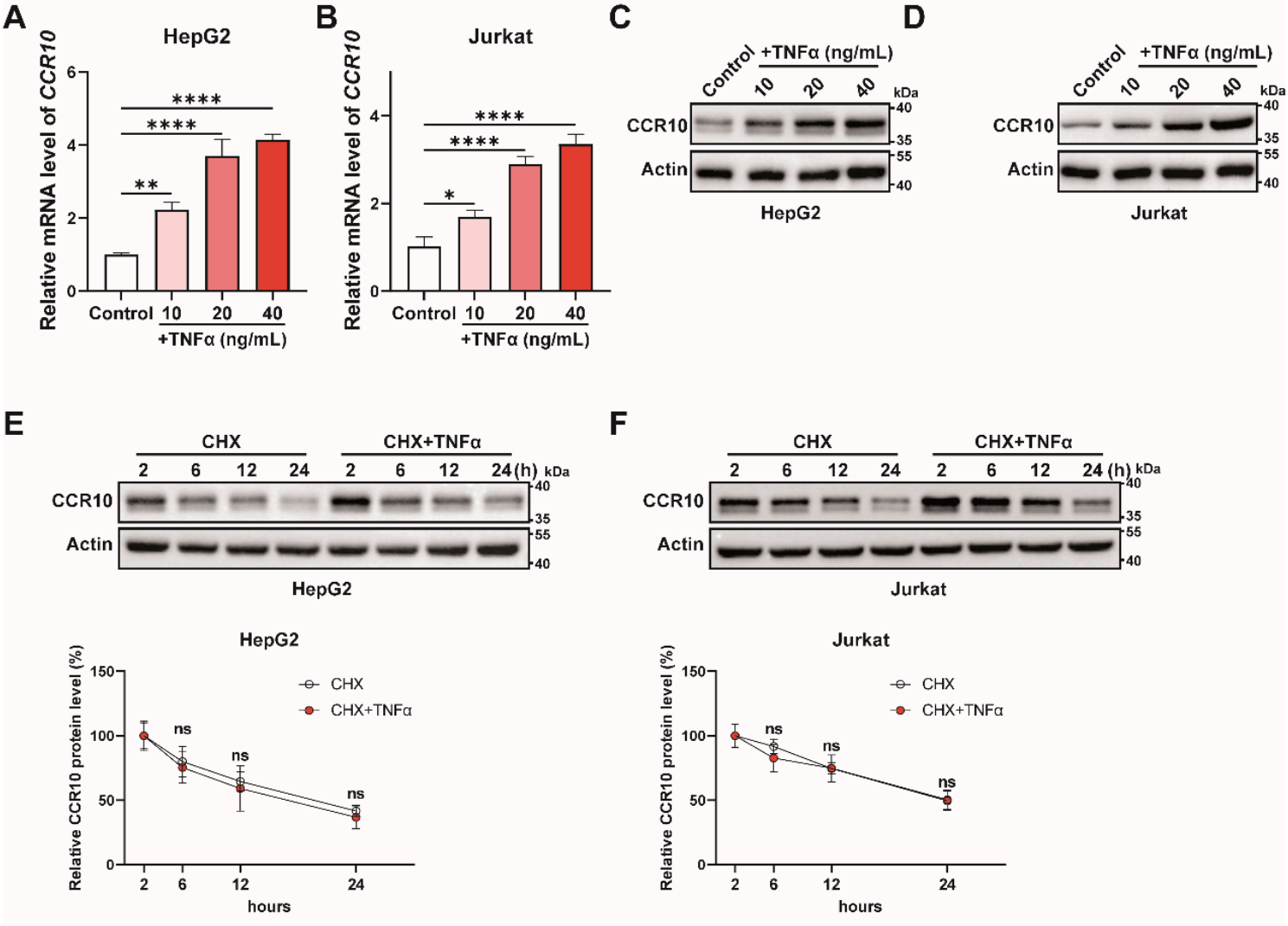


Figure 2

TNF-α upregulates CCR10 expression in HepG2 and Jurkat cells at the transcriptional level.

(A,B) qPCR analysis of *CCR10*mRNA in HepG2 (A) and Jurkat (B) cells after stimulation with the indicated concentrations of TNF-α; expression increased in a dose-dependent manner. (C,D) Western blot showing CCR10 protein levels in HepG2 (C) and Jurkat (D) cells treated with increasing TNF-α

concentrations. (E,F) Cells were treated with cycloheximide (CHX, 50 μg/mL) alone or combined with TNF-α; CCR10 protein decay was monitored by Western blot, and half-life curves showed no significant difference between groups, indicating TNF-α acts at the transcriptional level. Data are mean ± SD of three independent experiments. *P < 0.05 vs. 0 ng/mL TNF-α group.

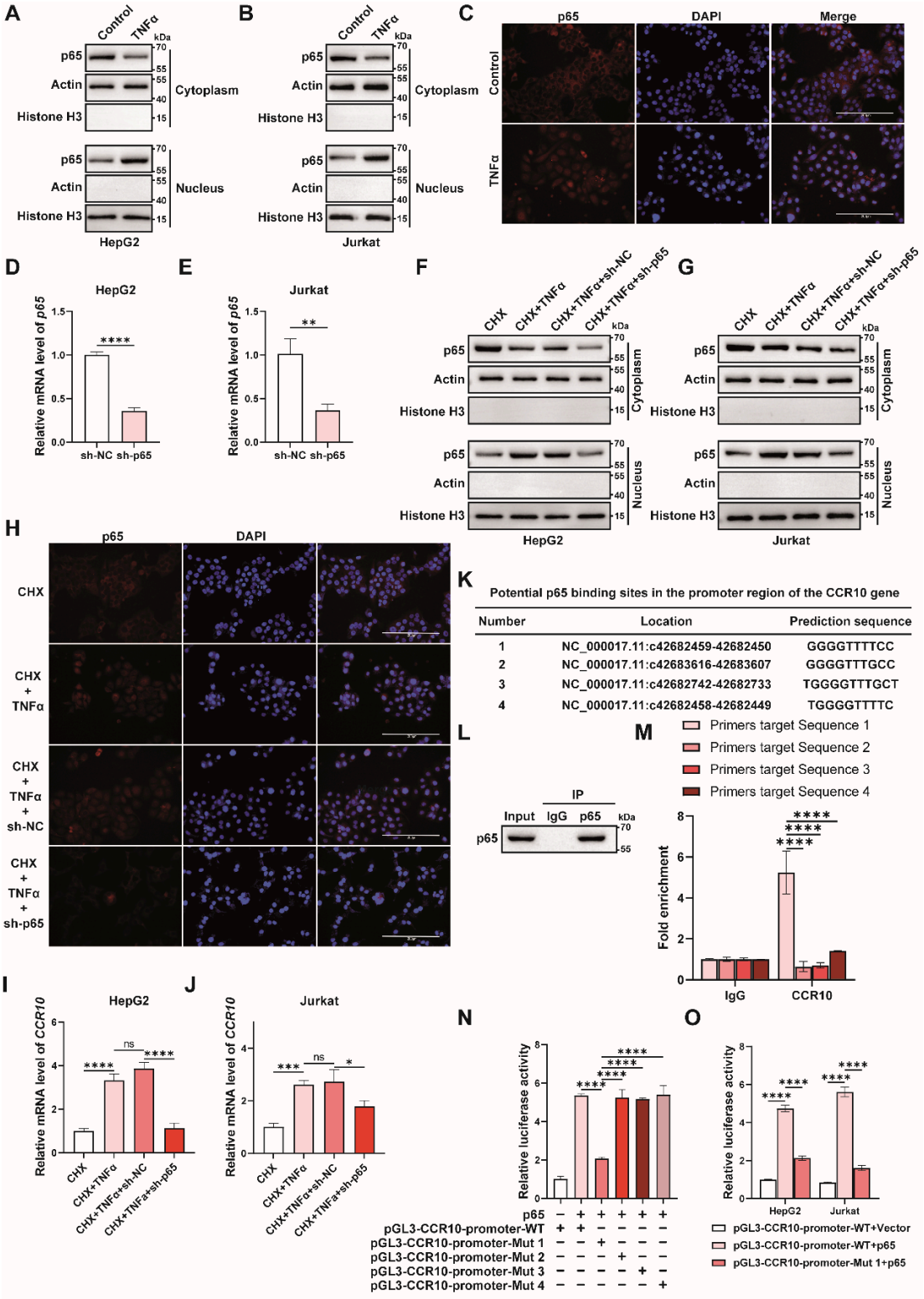


Figure 3

NF-κB/p65 is activated by TNF-α and directly binds the CCR10 promoter to drive transcription.

(A,B) Western blot of nuclear and cytoplasmic fractions showing p65 accumulation in the nucleus after TNF-α stimulation in HepG2 (A) and Jurkat (B) cells. (C) Immunofluorescence staining of p65 (green) in HepG2 cells; TNF-α induced translocation of p65 from the cytoplasm to the nucleus (DAPI, blue). (D,E) qPCR confirmation of p65 knockdown efficiency by shRNA in HepG2 (D) and Jurkat (E) cells. (F,G) Western blot showing reduced nuclear p65 in sh-p65–transfected cells stimulated with TNF-α (HepG2 shown; Jurkat similar). (H) Immunofluorescence confirming reduced nuclear p65 after p65 knockdown. (I,J) qPCR showing significant downregulation of *CCR10*mRNA in both HepG2 (I) and Jurkat (J) cells upon p65 knockdown. (K) Schematic of predicted p65-binding sites in the *CCR10*promoter (−2000 to +1 bp relative to TSS). (L) Chromatin immunoprecipitation (ChIP) assay showing enrichment of the *CCR10*promoter fragment by anti-p65 antibody in Jurkat cells. (M) Western blot of ChIP input and immunoprecipitated p65. (N) Dual-luciferase reporter assay with wild-type (WT) or mutated (Mut) *CCR10*promoter constructs; mutation of the p65-binding site abolished TNF-α/NF-κB–induced promoter activity in both HepG2 and Jurkat cells. Data are mean ± SD of three independent experiments. *P < 0.05 vs. control or WT.

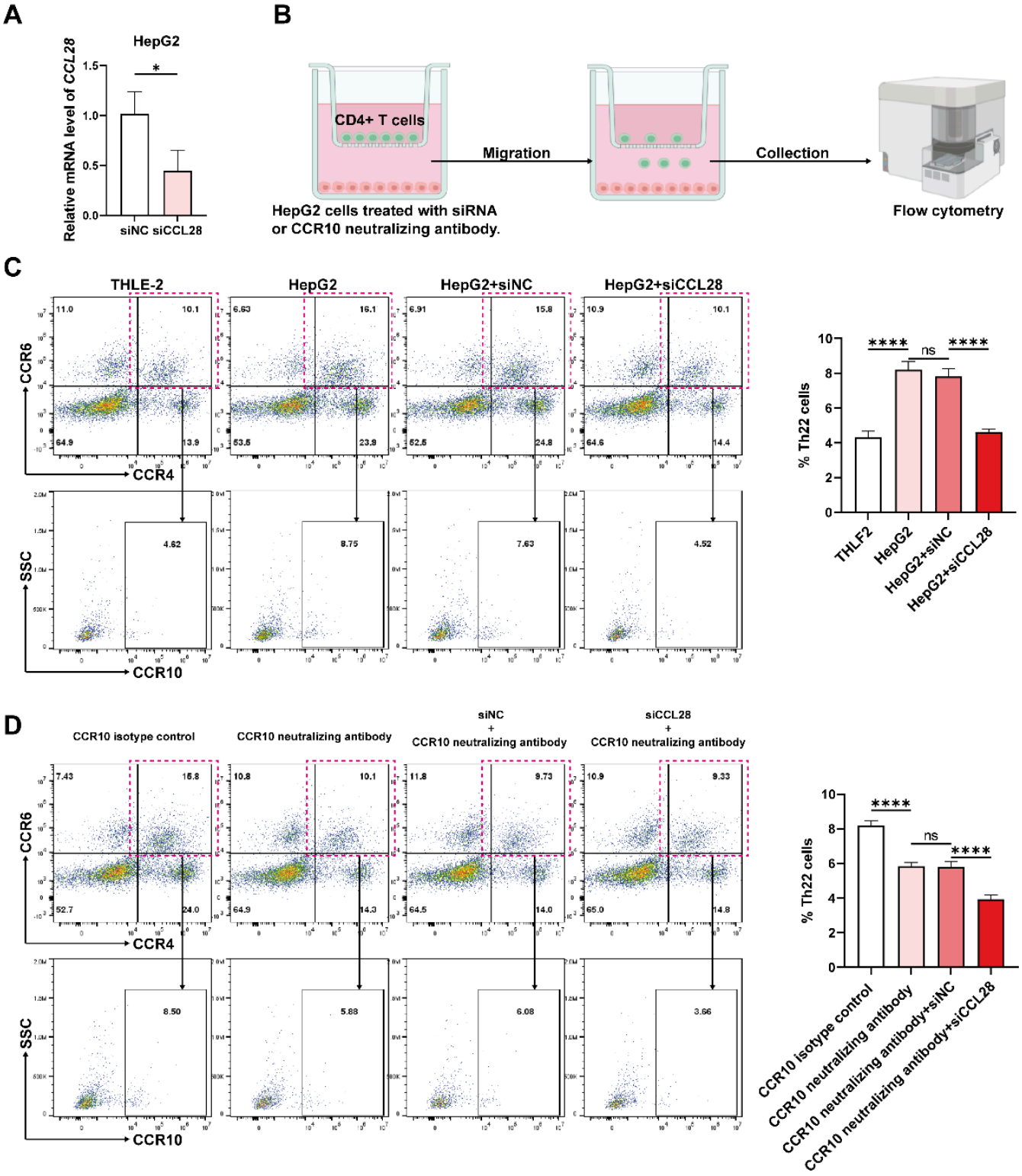


Figure 4

HCC cells recruit Th22 cells via CCL28–CCR10 interaction.

(A) qPCR verification of CCL28 knockdown efficiency in HepG2 cells transfected with si-CCL28. (B) Schematic of the Transwell migration assay: CD4⁺ T cells (upper chamber) were allowed to migrate toward HCC cells or controls (lower chamber). (C) Migrated Th22 cell proportion was significantly

increased when HepG2 cells were in the lower chamber compared with normal hepatocyte (LO2) control, and this increase was abrogated by CCL28 knockdown in HepG2 cells. (D) Neutralizing CCR10 on $CD4^+$ T cells or knocking down CCL28 in HepG2 cells similarly reduced Th22 cell migration; combined treatment did not further reduce migration. Data are representative of three independent experiments. *P < 0.05 vs. LO2 group; #P < 0.05 vs. HepG2 group.